5218 *Biochemistry* **2009,** *48,* 5218–5225
DOI: 10.1021/bi900415t

BIOCHEMISTRY
including biophysical chemistry & molecular biology
*Article*

# Crystal Structure of the Periplasmic Region of MacB, a Noncanonic ABC Transporter[†,‡]

Yongbin Xu,[§] Se-Hoon Sim,[#] Ki Hyun Nam,[⊥] Xiao Ling Jin,[§] Hong-Man Kim,[#] Kwang Yeon Hwang,[⊥] Kangseok Lee,[#] and Nam-Chul Ha*[,§]

[§]*College of Pharmacy and Research Institute for Drug Development, Pusan National University, Busan 609-735, Republic of Korea,* [#]*Department of Life Science, Chung-Ang University, Seoul 156-756, Republic of Korea, and* [⊥]*Division of Biotechnology and Genetic Engineering, College of Life and Environmental Sciences, Korea University, Seoul 136-791, Republic of Korea*

*Received March 10, 2009; Revised Manuscript Received May 9, 2009*

ABSTRACT: MacB is a noncanonic ABC-type transporter within Gram-negative bacteria, which is responsible both for the efflux of macrolide antibiotics and for the secretion of heat-stable enterotoxin II. In *Escherichia coli*, MacB requires the membrane fusion protein MacA and the multifunctional outer membrane channel TolC to pump substrates to the external medium. Sequence analysis of MacB suggested that MacB has a relatively large periplasmic region. To gain insight into how MacB assembles with MacA and TolC, we determined the crystal structure of the periplasmic region of *Actinobacillus actinomycetemcomitans* MacB. Fold matching program reveals that parts of the MacB periplasmic region have structural motifs in common with the RND-type transporter AcrB. Since it behaved as a monomer in solution, our finding is consistent with the dimeric nature of full-length MacB, providing an insight into the assembly in the tripartite efflux pump.

Because Gram-negative bacteria have two membrane layers, special transport systems are required to import and export nutrients, proteins, and toxic compounds (*1*, *2*). In particular, tripartite transport pumps are a typical system in Gram-negative bacteria (*3*). Of these pumps, *Escherichia coli* AcrA−AcrB−TolC, the major multidrug resistance pump, has been extensively studied (*2*, *4*−*7*). The homotrimeric AcrB is a resistance-nodulation-cell division (RND)[1]-type transporter located in the inner membrane, which pumps out diverse toxic compounds using a proton gradient across the membrane (*6*, *8*−*10*). The outer membrane factor (OMF) TolC in the tripartite pump provides a channel which traverses the outer membrane (*11*, *12*) in *E. coli*. The third essential component AcrA belongs to the family of membrane fusion proteins (MFPs) and connects AcrB to the central channel of TolC in *E. coli* (*4*, *13*, *14*).

Recently, a tripartite MacA-MacB-TolC pump and its homologues were identified in various Gram-negative bacteria. In *E. coli*, MFP MacA connects MacB and TolC (*15*−*18*). MacB was first identified as a macrolide antibiotic-specific transporter in *E. coli*, where it belongs to the family of ATP-binding cassette (ABC)-type transporters that utilize ATP hydrolysis as a driving force (*15*, *16*). It has been recently reported that MacB can also pump out heat-stable enterotoxin II (STII) in *E. coli* (*19*). Notably, MacB has a novel architecture, consisting of a four transmembrane segment, an N-terminal nucleotide binding domain (NBD), and a large periplasmic domain (*15*, *16*). Unlike MacB, most dimeric ABC-type transporters consist of six transmembrane segments, a C-terminal NBD, and a very small periplasmic region (*20*).

Full-length MacB is characterized as a homodimeric protein, revealed by nondissociating mass spectrometry, analytical ultracentrifugation, and atomic force microscopy (*21*). MacA is strictly required for the function of MacB in vivo (*15*), and MacA directly binds to MacB, which enhances the ATPase activity and macrolide-binding ability of MacB (*21*, *22*). However, it is largely unknown how MacA and MacB interact at the molecular level. MacA is anchored to the inner membrane via a single-spanning N-terminal transmembrane segment, which may be essential for the binding of MacB (*22*) despite controversial observations (*21*). Our research group recently revealed that MacA from the pathogenic bacterium *Actinobacillus actinomycetemcomitans* forms a funnel-shaped hexamer in vitro, which suggested that MacA is in a hexameric arrangement in its functional state (*23*).

Direct binding of TolC to MacB was detected using a pull-down assay in vitro (*21*). Compared to the interactions of MacA with both MacB and TolC, the interaction of TolC and MacB was much weaker, which was barely detectable using a specific antibody (*21*). Thus, it is still unclear whether the direct interaction of MacB and TolC is important for the function of the tripartite pumps. To obtain insight into how MacB operates and how MacB is assembled in the MacA-MacB-TolC pump, we

[†]This work was supported by the Bio-Scientific Research Grant funded by the Pusan National University (PNU, Bio-Scientific Research Grant; PNU-2008-0596-000) to N.-C.H.

[‡]The coordinates and structure factors of the Aa MacB PCD structure have been deposited into the Protein Data Bank (PDB code: 3FTJ).

*To whom correspondence should be addressed. Tel: +82 51 510 2528; fax: +82 51 513 6754; e-mail: hnc@pusan.ac.kr.

[1]Abbreviations: Mac, macrolide-specific ABC-type efflux carrier; ABC, ATP-binding cassette; RND, resistance-nodulation-cell division; OMF, outer membrane factor; GST, glutathione-S-transferase; PCD, periplasmic core domain.

 Published on Web 05/11/2009 

determined the crystal structure of the periplasmic region of MacB.

## EXPERIMENTAL PROCEDURES

*Overexpression and Purification of the Recombinant MacB PCD Proteins*. DNA fragments encoding *E. coli* MacB (residues 297−522) and *A. actinomycetemcomitans* MacB (residues 306−531) were ligated into the *NcoI* and *XhoI* sites of the pPROEX-HTA vector (Invitrogen, USA). Each recombinant MacB protein was expressed cytosolically as a hexa-histidine-tag fusion protein in the *E. coli* strain BL21 (DE3). Protein expression was induced by adding 0.5 mM isopropyl-$\beta$-D-1-thiogalactopyranoside (IPTG). The cells were harvested by centrifugation at 5000*g* for 30 min at 4 °C. Harvested cells were suspended in a lysis buffer containing 20 mM Tris (pH 8.0) and 150 mM NaCl and disrupted by sonication. The lysate was centrifuged at 45000*g* for 30 min at 4 °C. The resulting supernatant was loaded onto Ni-NTA agarose resin pre-equilibrated with the lysis buffer. The resin was washed with the lysis buffer supplemented with 20 mM imidazole and then eluted with the lysis buffer supplemented with 200 mM imidazole. The fractions containing the MacB protein were pooled, and 2-mercaptoethanol was added to a final concentration of 10 mM. This solution was incubated with recombinant TEV protease overnight at 4 °C to remove the hexa-histidine tag. The reaction mixture was subsequently loaded onto a Q-anion exchange column (Hitrap-Q; GE Healthcare, USA) for further purification, and proteins were eluted from the column using a 0−1 M NaCl gradient in 20 mM Tris buffer (pH 8.0). The collected fractions containing the MacB protein were pooled, concentrated, and separated on a HiLoad Superdex 200 gel-filtration column (GE Healthcare, USA) pre-equilibrated with the lysis buffer. The purified protein was concentrated to 10 mg/mL in 20 mM Tris buffer (pH 8.0) containing 150 mM NaCl and stored frozen at −80 °C until use.

*Crystallization, Data Collection, and Structure Determination*. Native Aa MacB PCD was crystallized in a precipitation solution containing 0.1 M HEPES (pH 7.5), 1% PEG 400, and 2.0 M ammonium sulfate. The crystallization was performed in droplets containing 1 $\mu$L of the protein solution (10 mg/mL) and 1 $\mu$L of the precipitant solution. The droplets were equilibrated by the hanging-drop vapor diffusion method against 1 mL of the precipitant solution at 14 °C for two weeks. Selenomethionine-labeled Aa MacB PCD (10 mg/mL) was crystallized in a precipitation solution containing 0.1 M MES (pH 6.5), 0.01 M cobalt chloride, and 1.8 M ammonium sulfate using the same method described above. For cryoprotection, the Aa MacB PCD crystals were coated with the sticky oil Paratone-N. The data sets were collected on BL4A at Pohang Accelerator Laboratory with a CCD detector Quantum 315 (ADSC) at −100 °C. The diffraction data sets were processed and scaled with the HKL2000 package (*24*). The crystal belongs to the space group *R*32 with cell dimensions of $a = b = 108.4$ Å, and $c = 92.9$ Å. Initial phases were determined by the multiple-wavelength anomalous dispersion data set using selenomethionine-labeled Aa MacB PCD. Of three selenomethionine residues in the asymmetric unit, two selenium sites were found and used for phase calculation by the SOLVE program (*25*). Density modification using RESOLVE (*25*) resulted in an electron density map, which was suitable for model building. Model building was performed using the program COOT (*26*), and model refinement was conducted using the programs CNS 1.2 (*27*). The program PHENIX.REFINE (*28*) was applied at the final round of the model refinement. Crystallographic data statistics are summarized in Table 1. All figures were prepared with PYMOL (*29*).

*Size Exclusion Chromatography*. To determine the molecular weight of proteins, size-exclusion chromatography was performed at a room temperature (22 °C) at a flow rate of 0.5 mL/min on a Superdex S-200 HR 10/30 (GE Healthcare) equilibrated with 20 mM Tris buffer (pH 8.0) containing 150 mM NaCl and 2 mM 2-mercaptoethanol. Two hundred microliters of each protein (1 mg/mL) was injected to the column.

*Peptide Synthesis, Binding Assays Using the Peptide*. Peptides for inhibition assays were prepared by solid-phase synthesis. The amino acid sequence of the peptide is "VLFNSFITDFSMD," which is shown as the second periplasmic region of Aa MacB in Figure 1A. The N- and C-termini of all peptides were modified by formylation and amidation, respectively. The identity and purity of the synthesized peptides were confirmed by mass spectrometry. In order to see if the peptide could bind to the MacB PCD, the Aa MacB PCD protein sample (30 $\mu$g) alone and the mixture (10 $\mu$g) with the synthetic peptide were subjected to native electrophoresis. A fluorescence titration binding assay was also performed to detect the binding of the peptide to the MacB PCD. The fluorescence emission spectra of the MacB PCD (1 mg/mL) were measured at 320 nm after the excitation at 290 nm. Fluorescence was not quenched by adding aliquots of the synthetic peptide even at the final 3 mM concentration of the peptide.

*In Vitro Binding Assay for MacA and TdeA*. The recombinant Aa MacA proteins were expressed and purified as a hexa-histidine-tag fusion proteins in the *E. coli* strain BL21 (DE3), as previously reported (*23*). The periplasmic domain of *A. actinomycetemcomitans* TdeA was generated by substitution of the membrane-embedded domain with short linkers, as previously reported (*30*). TdeA is *A. actinomycetemcomitans* homologure of *E. coli* TolC. The DNA fragment encoding the N-terminal GST-tagged TdeA periplasmic domain was inserted into the *NdeI* and *Eco*RI sites of pGEX-TEV. The construction and purification methods for the periplasmic domain of *A. actinomycetemcomitans* MacA have been reported (*23*, *31*). The GST-fused *A. actinomycetemcomitans* TdeA periplasmic region was purified using a glutathione-affinity chromatographic resin. The resin, bound to GST-fused TdeA protein, was incubated with *A. actinomycetemcomitans* MacA and/or Aa MacB PCD at 4 °C for 30 min. The resin was extensively washed with 20 mM Tris (pH 8.0) buffer containing 100 mM NaCl, and eluted with the same buffer supplemented with 20 mM glutathione. The eluted fractions were analyzed by SDS−PAGE, and the protein bands were stained with Coomassie blue.

## RESULTS AND DISCUSSION

*Structural Determination of the MacB Periplasmic Core Domain*. Because of the great difficulty of determining the structure of transmembrane proteins, we decided to determine the structure of the periplasmic region of MacB as an alternative to the full-length MacB protein. In accordance with its membrane topology, as determined by a competitive site-directed chemical modification (*16*), two putative periplasmic regions in the *E. coli* MacB (Ec MacB) amino acid sequence (Figure 1, residues 297−522 and residues 596−608) were selected. Only the first region (226 residues) was expected to form a structured

Table 1: X-ray Data Collection and Refinement Statistics

| | | Se-Met | | |
|---|---|---|---|---|
| data set | native | peak | edge | remote |
| wavelength (Å) | 1.0000 | 0.97943 | 0.97963 | 0.97175 |
| resolution limit (Å) | 50 − 2.0 (2.07 − 2.00)[a] | | 50 - 2.3 (2.38 − 2.3) [a] | |
| space group | *R*32 | | *R*32 | |
| unit cell (Å) | $a = b = 108.4$, $c = 92.9$ Å | | $a = b = 109.6$ Å, $c = 91.3$ Å | |
| reflections | | | | |
| unique | 13829 | 17294 | 17027 | 15988 |
| redundancy | 5.2 (2.6) | 3.2 (2.4) | 2.8 (2.1) | 2.4 (1.7) |
| $R_{merge}$[b](%) | 8.0 (32.1) | 4.3 (22.4) | 4.6 (29.4) | 4.6 (25.6) |
| completeness (%) | 96.3 (76.0) | 95.2 (87.9) | 93.7 (85.4) | 87.9 (58.0) |
| average $I/\sigma$ | 17.6 (2.1) | 27.6 (2.9) | 25.5 (2.7) | 18.4 (2.1) |
| refinement | | | | |
| resolution range (Å) | | | | 50 − 2.0 |
| *R*-factor (%) | | | | 19.9 |
| $R_{free}$[c] (%) | | | | 25.0 |
| average B value (Å$^2$) | | | | 31.4 |
| total number of atoms | | | | 1790 |
| number of water molecules | | | | 139 |
| rmsd for bonds (Å) | | | | 0.011 |
| rmsd for angles (°) | | | | 1.291 |
| Ramachandran plot | | | | |
| most favored | | | | 89.4% |
| additionally favored | | | | 9.0% |
| generously favored | | | | 1.1% |
| disallowed | | | | 0.5% |

[a] The numbers in parentheses are statistics for the highest resolution shell. [b] $R_{merge} = \Sigma_{hkl}\Sigma_i|I_{hkli} - \langle I_{hkli}\rangle|/\Sigma_{hkl}\Sigma_i\langle I_{hkli}\rangle$. [c] $R_{free}$ was calculated with 10% of the data set.

domain; the second region consists of only 13 residues, which seemed to be too short to form a structured motif.

The first region of Ec MacB was named a periplasmic core domain (PCD) and was overexpressed in *E. coli* cells for purification. In parallel, the corresponding region of *A. actinomycetemcomitans* MacB (Aa MacB; sequence similarity in PCD 57%) was identified by a sequence alignment to Ec MacB, and was also overexpressed in *E. coli* (Figure 1A). The structural integrity of the MacB PCD was confirmed by circular dichroism spectroscopy (Figure 1B). Crystallization trials for both MacB PCDs were successful, but only the crystals of Aa MacB PCD were suitable for data collection. Data were collected from a crystal of selenomethionine-substituted Aa MacB PCD protein, which allowed us to determine an electron density map by the multiple anomalous dispersion method. The resulting model of Aa MacB PCD consists of 208 residues, comprising 92% of the total number of amino acid residues in the crystallized protein. The Matthews coefficient ($V_M$) of the crystal was 2.07 Å$^3$ Da$^{-1}$ and the solvent content was calculated to be 41%.

*Overall Structure of Aa MacB PCD*. The asymmetric unit of the crystal contains one molecule of Aa MacB PCD (Figure 2A,B). The Aa MacB PCD consists of two distinct components: N- and C-terminal regions and a mixed $\alpha\beta$ domain. The two components are positioned perpendicularly, showing a sickle shape. The average temperature factors of the two components suggest that the N- and C-terminal regions are flexible (average B factor 50.3 Å$^2$), while the mixed $\alpha\beta$ domain is largely rigid (average B factor 28.6 Å$^2$). Although the N- and C-terminal flexible regions are located close to one another, physical contract was not observed between them. The N- and C-terminal regions are connected to the mixed $\alpha\beta$ domain via flexible linkers, and no interaction was observed between the N- and C-terminal regions and the mixed $\alpha\beta$ domain. The mixed $\alpha\beta$ domain consists of a nine-stranded $\beta$-sheet and three α-helices (Figure 2C). Notably, a shallow crevice was found in a middle of the mixed $\alpha\beta$ domain, where many bound water molecules were observed (Figure 2A,D). This crevice can virtually divide the domain into two parts: the upper and lower subdomains (Figure 2).

The MacB PCD is connected through the N- and C-terminal regions to the transmembrane segments in the full-length MacB, where the N-terminal flexible linker is linked to TM1 and the C-terminal α helix is connected to TM2 (Figure 2C). Motion of the NBD driven by ATP hydrolysis in the cytoplasm should be propagated to the periplasmic region of MacB through TM1 and TM2, in which the N- and C-terminal regions of PCD may play an important role.

Both the predicted and measured membrane topologies of MacB suggest that the two regions that were examined are putative periplasmic regions (*15*, *16*). To examine whether the short second periplasmic region is able to bind the MacB PCD, we analyzed binding using electrophoresis under nondenaturing conditions, and a fluorescence titration binding assay. No binding was detected between MacB PCD and the short second periplasmic region (data not shown).

*Structural Resemblance of MacB PCD to the AcrB Periplasmic Domain*. To find known structures similar to that of the MacB PCD, the fold match program DALI (*32*) was employed, and it suggested many candidates. Of these, the RND-type multidrug efflux transporter AcrB (PDB code: 2J8S) was indicated as the top match (Z-score 7.1). AcrB is a homotrimer, and each protomer consists of the TolC-docking domain (or a substrate exit domain) and the porter domain (*8*)

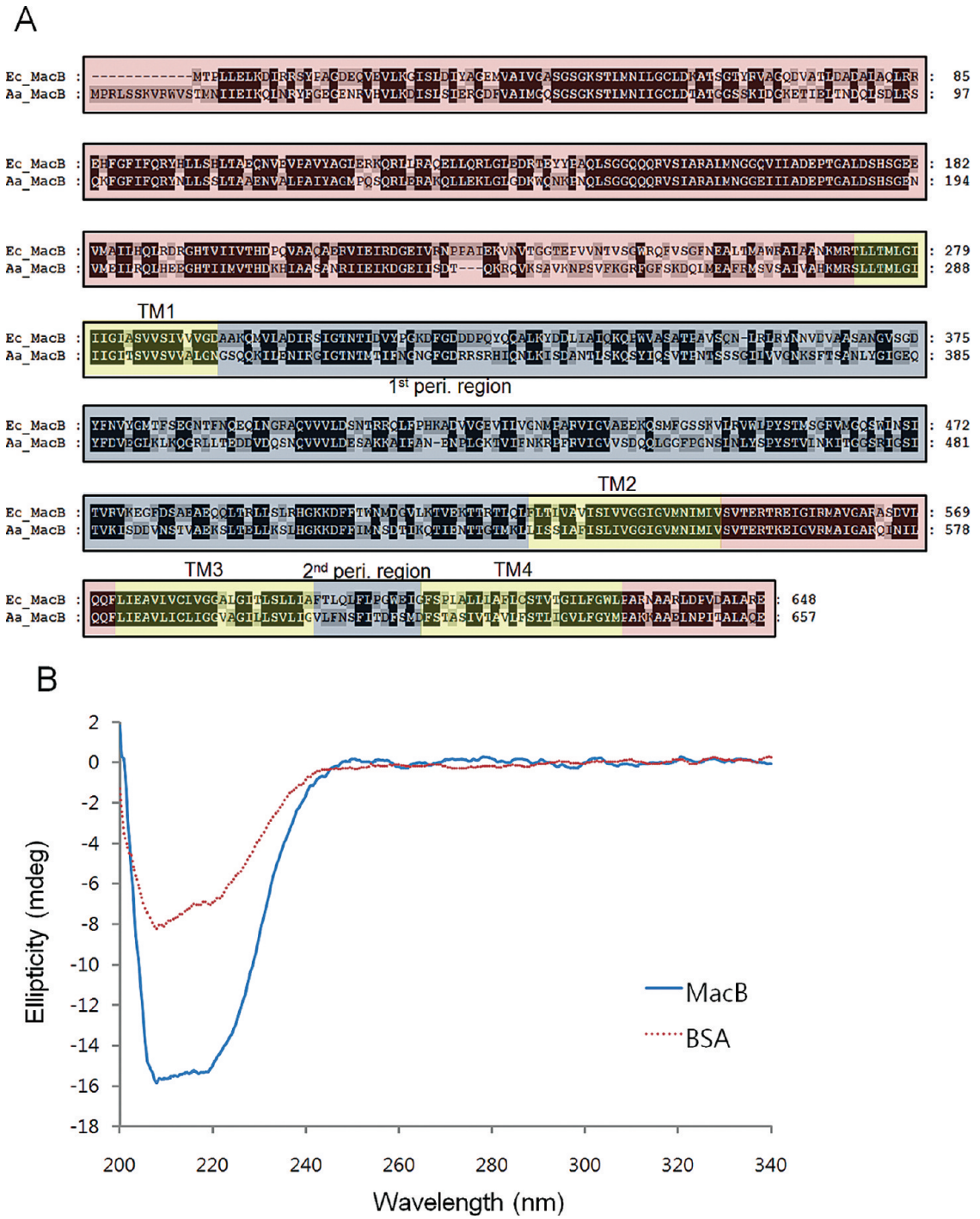


FIGURE 1: Putative periplamic region of MacB proteins. (A) Sequence alignment of Ec MacB and Aa MacB. The intracellular regions, transmembrane segments, and periplasmic regions are indicated by red, yellow, and blue boxes, respectively. The nucleotide binding domain (NBD) is located in the N-terminal intracellular region, and four transmembrane segments are labeled above the sequences (TM1−TM4). The two periplasmic regions (1st peri. region and 2nd peri. region) are indicated in the sequence or above the sequence. The sequence alignment was carried out using the program BL2SEQ in BLAST. (B) Circular dichroism spectra of Aa MacB PCD (MacB) and bovine serum albumin (BSA). The concentration of each protein is 0.2 mg/mL in 20 mM Tris buffer (pH 8.0) containing 150 mM NaCl and 2-mercapthanol. CD spectrum was recorded on a JASCO J-810 spectropolarimeter. Spectra were collected from 340 to 200 nm at an interval of 1 nm and 3 accumulations.

(Figure 3A). A substrate binding pocket exists in the porter domain of each protomer, and the porter domain consists of four subdomains whose overall architectures are similar (*8*). Structural comparison of the MacB PCD to AcrB suggested that the overall structural architecture of the lower subdomain of MacB PCD is similar to those of subdomains of the AcrB porter domain (Figure 3B). The DALI (*32*) showed Z-score 7.3 and rmsd 3.7 Å between the lower subdomain of MacB PCD (87 Cα positions) and the AcrB porter domain (110 Cα positions). Furthermore, additional structural similarity was found between the tip region in the upper subdomain of the MacB PCD and the tip region of the AcrB substrate exit domain, which are characterized as a $\beta$-hairpin and a short α-helix (Figure 3C). Since the tip region of AcrB is involved in the pump assembly (*8*, *10*, *33*), these regions may also play a role in forming similar structures in the cognate binding partners of MacB.

*MacB Periplasmic Regions Do Not Have a Strong Affinity toward Each Other*. To examine the oligomeric state

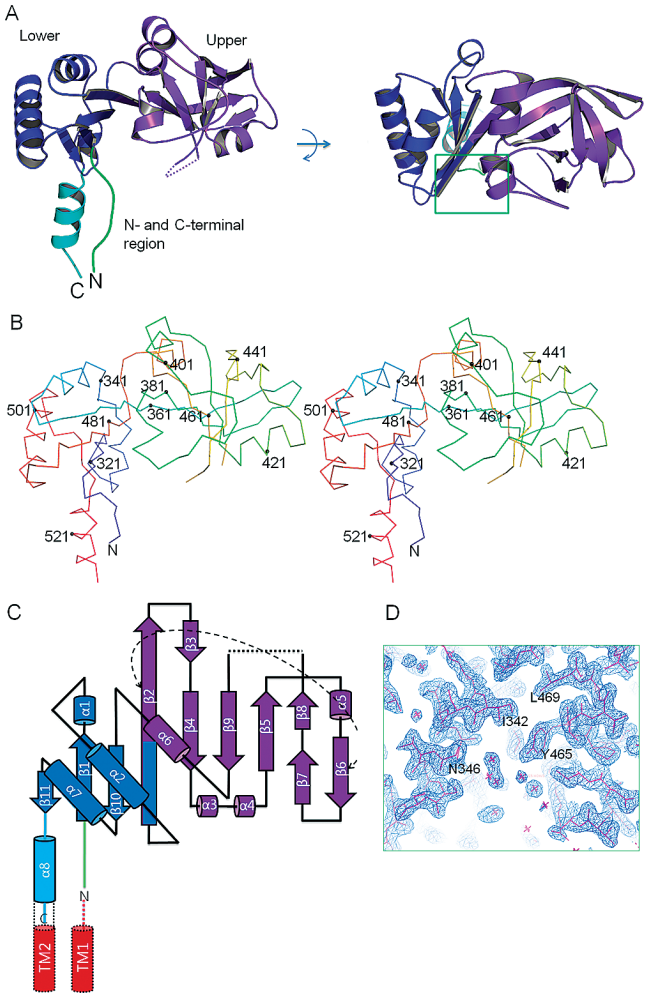


FIGURE 2: The overall structure of the MacB PCD. (A) Ribbon representations of the asymmetric unit of the Aa MacB PCD. A side view and a top view are depicted. The N- and C-terminal regions are shown in green and cyan, respectively. The upper and lower subdomains of the mixed $\alpha\beta$ domain are shown in violet and blue, respectively. The green box indicates the crevice between the upper and lower subdomains, a close-up view of which is shown in (D). (B) Stereo view of the Cα trace of the asymmetric unit. Every 20 amino acid is labeled with its residue number. (C) Folding topology of the Aa MacB PCD, depicted in the same color scheme as (A). Imaginary transmembrane segments 1 and 2 (TM1, TM2) are displayed in red cylinders. (D) A close up view of the crevice region with its electron density map ($2F_o - F_c$ map contoured at $1\sigma$).

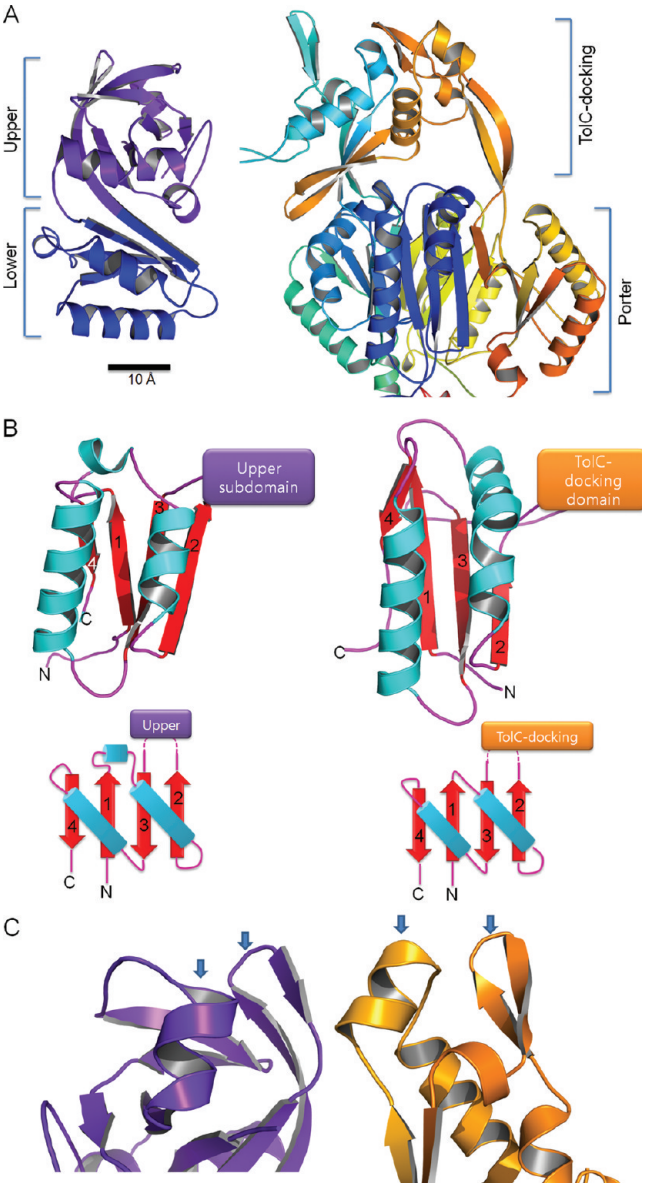


FIGURE 3: Structural comparison of MacB to AcrB. (A) Secondary structures of periplasmic regions of MacB (Left) and AcrB (Right, PDB code 2J8S). Given a scale bar, the relative size of MacB to AcrB can be compared. (B) Lower subdomain of MacB (Left) and a subdomain of the AcrB porter domain (Right), showing with their folding topologies. Note that the protein folds and overall structures are similar. (C) The periplasmic tip regions of MacB and AcrB, highlighting the α-helix and the $\beta$-hairpin. The arrows indicate the α-helix and $\beta$-hairpin, which are characteristic of the tip regions.

of the MacB PCD in solution, we measured the molecular sizes of Aa MacB PCD and Ec MacB PCD proteins using size exclusion chromatography. The results showed that both MacB PCD proteins behaved as monomers in solution (Figure 4), suggesting that the subunits of the MacB PCD do not have a strong affinity toward each other. Since the full-length MacB protein is a dimer (*21*), the MacB PCD subunits should be close together in vivo even though the MacB PCD does not make direct contact. This suggests a structural model for the full-length MacB protein, which is analogous to canonical ABC-type exporters, such as Sav1866 and MsbA (*34*, *35*), although MacB is different from canonical ABC-type exporters that have a small extracellular domain. The canonical ABC-type exporters have a cavity for substrate exit at the center of the two subunits. In the model of the full-length MacB protein, two MacB PCD subunits face each other, where the MacB tip regions resembling AcrB substrate exit regions orient upward. This model suggests that the tip region of the MacB PCD may be involved in docking with MacA or TolC, a functionality that is comparable to that of AcrB. Since the substrate exit region of AcrB was proposed to be linked to the periplasmic entry site of TolC through the $\beta$-hairpin motifs, the corresponding region of the MacB PCD may act as a docking motif to the cognate binding partner in vivo.

Since STII is released into the periplasm through the Sec machinery as seen in the type II secretory process, it was suggested that MacB should take up STII in the periplasm in order to pump it out (*19*). The porter domain of AcrB forms a substrate entrance site, and its conformation change is coupled with proton translocation (*8*−*10*). Given the structural similarity of the lower subdomain of MacB to the porter domain of AcrB, it is tempting to suggest that the lower subdomain of MacB may

form a substrate entrance site in its functional form, and its conformation is interlocked with the motion of the intracellular NBD. However, the full-length MacB structure is required to elucidate the mechanism of action of MacB.

*No Direct Interaction of the MacB PCD with the Outer Membrane Factor*. The periplasmic region of MacB has been believed to bind the periplasmic domain of the OMF TolC (*15*, *21*, *22*). To test whether the MacB PCD directly binds the periplasmic region of TolC, a binding assay was performed using purified proteins. Because the Aa MacB PCD was used in the binding assay, Aa TdeA (a TolC homologue of *A. actinomycetemcomitans* which has 21% sequence identity to *E. coli* TolC; referred to as Aa TolC hereafter) was employed. To exclude the possibility that added detergent in the reaction buffer might interfere with protein−protein interaction, we produced a detergent-free in vitro binding assay system, because all the proteins lack the integral membrane region. In this assay, we employed the transmembrane segment-deleted versions of Aa TolC protein and Aa MacA. We previously confirmed that the transmembrane segment-deleted Aa TolC protein is correctly folded in vitro (*30*). As shown in Figure 5A, the GST-fused Aa TolC periplasmic domain was not bound to the MacB PCD, which is in sharp contrast to the strong binding of Aa TolC to Aa MacA. Moreover, the TolC−MacA complex failed to recruit the MacB PCD. These observations indicate that the MacB PCD is not directly associated with TolC, and are also consistent with a previous report using full-length *E. coli* proteins, in which MacB-TolC binding was much weaker than MacA-TolC binding (*21*). Our in vitro assay result showing the inability of the periplasmic regions of MacA to bind MacB was somewhat predicted by the previous finding that the transmembrane segments of both proteins were required for binding and functionality (*22*).

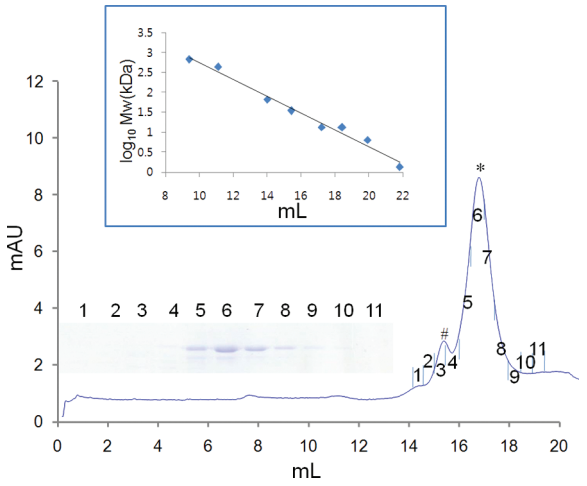


FIGURE 4: Size exclusion chromatography of the MacB PCD. The purified protein of the Aa MacB PCD was subjected to size exclusion chromatography. When the standard size markers indicated by arrows are considered, the molecular weight of the peak (*) was calculated as ~20 kDa, which is well matched to the calculated molecular weight of the MacB PCD (24.8 kDa). The surrounding peak (#) does not contain the protein, as seen in the SDS−polyacrylamide gel analyzing each fraction. The inset shows the elution volumes of eight different standard proteins, and the straight line represents a linear fit. The Ec MacB PCD showed a similar elution profile (data not shown).

*An Insight into the Assembly of the Tripartite Macrolide-Specific Efflux Pump*. An assembly model for the tripartite AcrA-AcrB-TolC pump has been proposed, where the inner membrane component AcrB directly interacts with OMF TolC, and AcrA wraps the outsides of the TolC and AcrB periplasmic regions (*33*, *36*). The model has been supported by detection of AcrB-TolC cross-linked adducts in vivo and in vitro (*33*), and the complementary structure of the tip regions of AcrB and TolC (*8*). A similar assembly model for the MacA-MacB-TolC pump has been proposed by others (*15*, *21*, *22*), in which MacB makes direct contact with the substrate entry site of TolC (designated as "TolC-docking model"). However, this model is not supported by our observation that the Aa TolC protein has no affinity to the

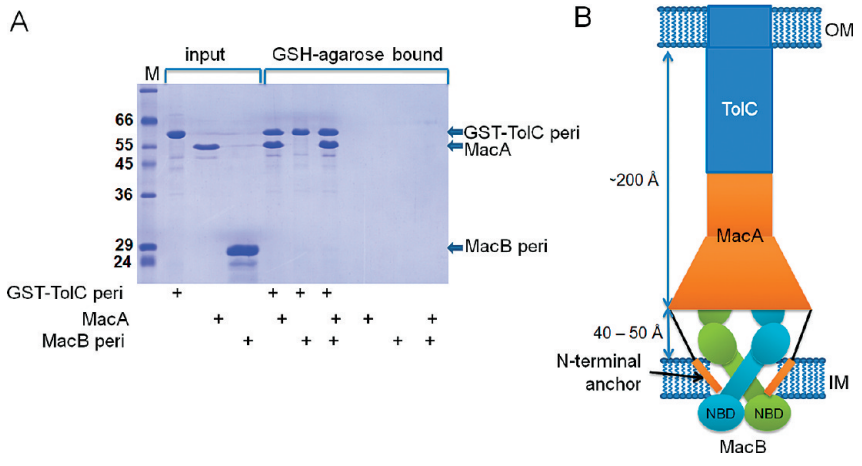


FIGURE 5: Interactions between MacA, MacB, and TolC. (A) In vitro binding assay for the periplasmic regions of TolC, MacA, and MacB. The GST-fused TolC periplasmic region (GST-TolC peri) was preincubated with GSH-agarose beads, and washed to remove unbound proteins. Then, the MacA and/or MacB periplasmic regions were incubated with GST-fused TolC bound resins or GSH-agarose resin itself. Finally, the bound proteins were analyzed on an SDS−polyacrylamide gel. Positions of molecular markers (kDa) are shown on the left. All proteins are from *A. actinomycetemcomitans*. (B) A structural model (MacA-bridging model) of the tripartite MacA-MacB-TolC pump. The funnel-like MacA hexamer docks to TolC via tip-to-tip interaction. The periplasmic part of MacB is accommodated by the hollow adjacent to the inner membrane (IM). Although the intracellular NBD contributes to the dimerization of MacB, the periplasmic region of MacB does not contribute to dimerization. The N-terminal transmembrane segments of MacA (MacA N-terminal anchors) are shown in rectangles in the inner membrane, which may be the major MacA-interacting moiety. This model does not allow for direct interaction between TolC and MacB. The complex spans the entire periplasmic space, inner membrane, and outer membrane (OM). The periplasmic parts of the MacA-TolC complex are approximately 200 Å long, and the MacB periplasmic regions are 40−50 Å long, depending on the extent of MacA binding.

periplasmic region of Aa MacB. Moreover, analysis of crystal packing and size exclusion chromatography of the MacB PCD found no propensity to form a higher-order oligomer, such as a trimer or dimer. Thus, the TolC-docking model would become geometrically unreasonable in the MacA−MacB−TolC pump since the homotrimeric TolC could not bind the homodimeric MacB. Taken together, we conclude from these results that the current prevailing model for the AcrA−AcrB−TolC pump is not applicable to the MacA−MacB−TolC pump.

Given that the TolC docking model is not supported by MacB structural and biochemical observations, how is the MacA−MacB−TolC pump assembled in vivo? We previously proposed a new assembly model based on the hexameric structure of MacA resembling a funnel, in which MacA forms a bridge between MacB and TolC (designated as "MacA-bridging model") (*23*). The MacA-bridging model highlights the role of MacA in opening the TolC channel and linking the other two components. In this MacA-bridging model, we speculate that the tip region of MacB fits into the funnel-mouth region of the MacA hexamer, and that the lower subdomain of MacB provides the substrate entrance site (Figure 5B). The MacA-bridging model also agrees well with the evidence of strong binding between MacA-TolC and MacA-MacB (*21*, *22*). To connect the trimeric TolC to the dimeric MacB, the oligomerization number of the bridging protein should be six or a multiple thereof, where the number six is chosen because it is the least common multiple of three and two. Thus, it is geometrically reasonable that the hexameric MacA connects the trimeric TolC to the dimeric MacB. However, further studies are needed to build an exact model for the MacA−MacB−TolC pump.

## ACKNOWLEDGMENT

This study made use of beamline 4A at Pohang Accelerator Laboratory (Pohang, Korea). The authors declare no competing financial interests.

## REFERENCES

1. Lewis, K. (2000) Translocases: a bacterial tunnel for drugs and proteins. *Curr. Biol. 10*, R678–681.
2. Zgurskaya, H. I., and Nikaido, H. (1999) Bypassing the periplasm: reconstitution of the AcrAB multidrug efflux pump of *Escherichia coli*. *Proc. Natl. Acad. Sci. U. S. A. 96*, 7190–7195.
3. Dinh, T., Paulsen, I. T., and Saier, M. H.Jr. (1994) A family of extracytoplasmic proteins that allow transport of large molecules across the outer membranes of gram-negative bacteria. *J. Bacteriol. 176*, 3825–3831.
4. Ma, D., Cook, D. N., Alberti, M., Pon, N. G., Nikaido, H., and Hearst, J. E. (1993) Molecular cloning and characterization of *acrA* and *acrE* genes of *Escherichia coli*. *J. Bacteriol. 175*, 6299–6313.
5. Nikaido, H. (1994) Prevention of drug access to bacterial targets: permeability barriers and active efflux. *Science 264*, 382–388.
6. Ma, D., Cook, D. N., Alberti, M., Pon, N. G., Nikaido, H., and Hearst, J. E. (1995) Genes *acrA* and *acrB* encode a stress-induced efflux system of *Escherichia coli*. *Mol. Microbiol. 16*, 45–55.
7. Okusu, H., Ma, D., and Nikaido, H. (1996) AcrAB efflux pump plays a major role in the antibiotic resistance phenotype of *Escherichia coli* multiple-antibiotic-resistance (Mar) mutants. *J. Bacteriol. 178*, 306–308.
8. Murakami, S., Nakashima, R., Yamashita, E., and Yamaguchi, A. (2002) Crystal structure of bacterial multidrug efflux transporter AcrB. *Nature 419*, 587–593.
9. Seeger, M. A., Schiefner, A., Eicher, T., Verrey, F., Diederichs, K., and Pos, K. M. (2006) Structural asymmetry of AcrB trimer suggests a peristaltic pump mechanism. *Science 313*, 1295–1298.
10. Murakami, S., Nakashima, R., Yamashita, E., Matsumoto, T., and Yamaguchi, A. (2006) Crystal structures of a multidrug transporter reveal a functionally rotating mechanism. *Nature 443*, 173–179.
11. Fralick, J. A. (1996) Evidence that TolC is required for functioning of the Mar/AcrAB efflux pump of *Escherichia coli*. *J. Bacteriol. 178*, 5803–5805.
12. Koronakis, V., Sharff, A., Koronakis, E., Luisi, B., and Hughes, C. (2000) Crystal structure of the bacterial membrane protein TolC central to multidrug efflux and protein export. *Nature 405*, 914–919.
13. Zgurskaya, H. I., and Nikaido, H. (1999) AcrA is a highly asymmetric protein capable of spanning the periplasm. *J. Mol. Biol. 285*, 409–420.
14. Zgurskaya, H. I., Yamada, Y., Tikhonova, E. B., Ge, Q., and Krishnamoorthy, G. (2009) Structural and functional diversity of bacterial membrane fusion proteins. *Biochim. Biophys. Acta 1798*, 794–807.
15. Kobayashi, N., Nishino, K., and Yamaguchi, A. (2001) Novel macrolide-specific ABC-type efflux transporter in *Escherichia coli*. *J. Bacteriol. 183*, 5639–5644.
16. Kobayashi, N., Nishino, K., Hirata, T., and Yamaguchi, A. (2003) Membrane topology of ABC-type macrolide antibiotic exporter MacB in Escherichia coli. *FEBS Lett. 546*, 241–246.
17. Rouquette-Loughlin, C. E., Balthazar, J. T., and Shafer, W. M. (2005) Characterization of the MacA-MacB efflux system in *Neisseria gonorrhoeae*. *J. Antimicrob. Chemother. 56*, 856–860.
18. Crosby, J. A., and Kachlany, S. C. (2007) TdeA, a TolC-like protein required for toxin and drug export in *Aggregatibacter (Actinobacillus) actinomycetemcomitans*. *Gene 388*, 83–92.
19. Yamanaka, H., Kobayashi, H., Takahashi, E., and Okamoto, K. (2008) MacAB Is Involved in the Secretion of *Escherichia coli* Heat-Stable Enterotoxin II. *J. Bacteriol. 190*, 7693–7698.
20. Davidson, A. L., Dassa, E., Orelle, C., and Chen, J. (2008) Structure, function, and evolution of bacterial ATP-binding cassette systems. *Microbiol. Mol. Biol. Rev. 72*, 317–364.
21. Lin, H. T., Bavro, V. N., Barrera, N. P., Frankish, H. M., Velamakanni, S., van Veen, H. W., Robinson, C. V., Borges-Walmsley, M. I., and Walmsley, A. R. (2008) The MacB ABC transporter is a dimer whose ATPase activity and macrolide-binding capacity are regulated by the membrane fusion protein MacA. *J. Biol. Chem. 284*, 1145–1154.
22. Tikhonova, E. B., Devroy, V. K., Lau, S. Y., and Zgurskaya, H. I. (2007) Reconstitution of the *Escherichia coli* macrolide transporter: the periplasmic membrane fusion protein MacA stimulates the ATPase activity of MacB. *Mol. Microbiol. 63*, 895–910.
23. Yum, S., Xu, Y., Piao, S., Sim, S. H., Kim, H. M., Jo, W. S., Kim, K. J., Kweon, H. S., Jeong, M. H., Jeon, H., Lee, K., and Ha, N. C. (2009) Crystal structure of the periplasmic component of a tripartite macrolide-specific efflux pump. *J. Mol. Biol. 387*, 1286–1297.
24. Otwinosky, Z., and Minor, W. (1997) Processing of X-ray diffraction data collected in oscillation mode. *Methods Enzymol. 276*, 307–326.
25. Terwilliger, T. C., and Berendzen, J. (1999) Automated MAD and MIR structure solution. *Acta Crystallogr. D Biol. Crystallogr. 55*, 849–861.
26. Emsley, P., and Cowtan, K. (2004) Coot: model-building tools for molecular graphics. *Acta Crystallogr. D Biol. Crystallogr. 60*, 2126–2132.
27. Brunger, A. T., Adams, P. D., Clore, G. M., DeLano, W. L., Gros, P., Grosse-Kunstleve, R. W., Jiang, J. S., Kuszewski, J., Nilges, M., Pannu, N. S., Read, R. J., Rice, L. M., Simonson, T., and Warren, G. L. (1998) Crystallography & NMR system: A new software suite for macromolecular structure determination. *Acta Crystallogr. D Biol. Crystallogr. 54*, 905–921.
28. Adams, P. D., Grosse-Kunstleve, R. W., Hung, L. W., Ioerger, T. R., McCoy, A. J., Moriarty, N. W., Read, R. J., Sacchettini, J. C., Sauter, N. K., and Terwilliger, T. C. (2002) PHENIX: building new software for automated crystallographic structure determination. *Acta Crystallogr. Sect. D Biol. Crystallogr. 58*, 1948–1954.
29. DeLano, W. (2002) The PyMOL User's Manual , DeLano Scientific, Palo Alto.
30. Kim, S., Yum, S., Jo, W. S., Lee, B. L., Jeong, M. H., and Ha, N. C. (2008) Expression and biochemical characterization of the periplasmic domain of bacterial outer membrane porin TdeA. *J. Microbiol. Biotechnol. 18*, 845–851.
31. Piao, S., Xu, Y., and Ha, N. C. (2008) Crystallization and preliminary X-ray crystallographic analysis of MacA from *Actinobacillus actinomycetemcomitans*. *Acta Crystallogr. Sect. F Struct. Biol. Cryst. Commun. 64*, 391–393.
32. Holm, L., and Sander, C. (1993) Protein structure comparison by alignment of distance matrices. *J. Mol. Biol. 233*, 123–138.

33. Tamura, N., Murakami, S., Oyama, Y., Ishiguro, M., and Yamaguchi, A. (2005) Direct interaction of multidrug efflux transporter AcrB and outer membrane channel TolC detected via site-directed disulfide cross-linking. *Biochemistry 44*, 11115–11121.
34. Hollenstein, K., Frei, D. C., and Locher, K. P. (2007) Structure of an ABC transporter in complex with its binding protein. *Nature 446*, 213–216.
35. Ward, A., Reyes, C. L., Yu, J., Roth, C. B., and Chang, G. (2007) Flexibility in the ABC transporter MsbA: Alternating access with a twist. *Proc. Natl. Acad. Sci. U. S. A. 104*, 19005–19010.
36. Bavro, V. N., Pietras, Z., Furnham, N., Perez-Cano, L., Fernandez-Recio, J., Pei, X. Y., Misra, R., and Luisi, B. (2008) Assembly and channel opening in a bacterial drug efflux machine. *Mol. Cell 30*, 114–121.